

# Deep Reinforcement Learning Guided Graph Neural Networks for Brain Network Analysis

Xusheng Zhao<sup>a,b</sup>, Jia Wu<sup>c</sup>, Hao Peng<sup>d,\*</sup>, Amin Beheshti<sup>c</sup>, Jessica Monaghan<sup>e</sup>, David McAlpine<sup>f</sup>, Heivet Hernandez-Perez<sup>f</sup>, Mark Dras<sup>c</sup>, Qiong Dai<sup>a,b,\*</sup>, Yangyang Li<sup>g</sup>, Philip S. Yu<sup>h</sup>, Lifang He<sup>i</sup>

<sup>a</sup>*Institute of Information Engineering, Chinese Academy of Sciences, Beijing, China*

<sup>b</sup>*School of Cyber Security, University of Chinese Academy of Sciences, Beijing, China*

<sup>c</sup>*Department of Computing, Macquarie University, NSW, Australia*

<sup>d</sup>*Beijing Advanced Innovation Center for Big Data and Brain Computing, Beihang University, Beijing, China*

<sup>e</sup>*National Acoustic Laboratories, NSW, Australia*

<sup>f</sup>*Department of Linguistics, Macquarie University, NSW, Australia*

<sup>g</sup>*National Engineering Laboratory for Risk Perception and Prevention (NEL-RPP), CAEIT, Beijing, China*

<sup>h</sup>*Department of Computer Science, University of Illinois at Chicago, IL, USA*

<sup>i</sup>*Computer Science & Engineering, Lehigh University, PA, USA*

## Abstract

Modern neuroimaging techniques, such as diffusion tensor imaging (DTI) and functional magnetic resonance imaging (fMRI), enable us to model the human brain as a brain network or connectome. Capturing brain networks' structural information and hierarchical patterns is essential for understanding brain functions and disease states. Recently, the promising network representation learning capability of graph neural networks (GNNs) has prompted many GNN-based methods for brain network analysis to be proposed. Specifically, these methods apply feature aggregation and global pooling to convert brain network instances into meaningful low-dimensional representations used for downstream brain network analysis tasks. However, existing GNN-based methods often neglect that brain networks of different subjects may require various aggregation iterations and use GNN with a fixed number of layers to learn all brain networks. Therefore, how to fully release the potential of GNNs to promote brain network analysis is still non-trivial. To solve this problem, we propose a novel brain network representation framework, namely BN-GNN, which searches for the optimal GNN architecture for each brain network. Concretely, BN-GNN employs deep reinforcement learning (DRL) to train a meta-policy to automatically determine the optimal number of feature aggregations (reflected in the number of GNN layers) required for a given brain network. Extensive experiments on eight real-world brain network datasets demonstrate that our proposed BN-GNN improves the performance of traditional GNNs on different brain network analysis tasks.

**Keywords:** Brain Network; Network Representation Learning; Graph Neural Network; Deep Reinforcement Learning.

## 1. Introduction

With recent advances in modern neuroimaging techniques, using neuroimaging data effectively has become a research hotspot in both academia and industry [1, 2]. Many of these techniques, such as diffusion tensor imaging (DTI) [1] and functional magnetic resonance imaging (fMRI) [2], enable us to model the human brain as a connectivity network (known as "brain network") [3, 4]. Unlike the brain image composed of pixels, the brain network is composed of nodes and edges. Nodes often represent regions of interest (ROIs) in the brain, and edges represent the connectivity or correlation between pairs of ROIs. There are often distinct differences between the brain networks derived from different imaging modalities [5]. For example, DTI-derived brain networks encode the structural connections among ROIs based on white matter fibers, while fMRI-derived brain networks record the functional activity routes of the regions. Both structural and functional brain networks have been extensively studied and applied to the whole-brain analysis.

The computational analysis of brain networks is becoming more and more popular in healthcare because it can discover meaningful structural information and hierarchical patterns to help understand brain functions and diseases. Here we take

\*Corresponding author

Email addresses: zhaoxusheng@iie.ac.cn (Xusheng Zhao), jia.wu@mq.edu.au (Jia Wu), penghao@buaa.edu.cn (Hao Peng), amin.beheshti@mq.edu.au (Amin Beheshti), jessica.monaghan@nal.gov.au (Jessica Monaghan), david.mcalpine@mq.edu.au (David McAlpine), heivet.hernandez-perez@mq.edu.au (Heivet Hernandez-Perez), mark.dras@mq.edu.au (Mark Dras), daiqiong@iie.ac.cn (Qiong Dai), liyangyang@cetc.com.cn (Yangyang Li), psyu@uic.edu (Philip S. Yu), lih319@lehigh.edu (Lifang He)

brain disease prediction as an example. As one of the most common diseases affecting human health, brain disease has a very high incidence and disability rate, bringing enormous economic and human costs to society [6]. Considering the complexity and diversity of the predisposing factors of brain diseases, researchers often analyze the brain network states of subjects to assist in inferring the types of brain diseases and then provide reliable and effective prevention or treatment guidelines. For example, Alzheimer's disease (AD) is a progressive neurodegenerative disease widespread in the elderly, mainly manifested as memory and visual-spatial skill impairments [7, 8]. Although the existing medical methods cannot effectively treat AD patients, it is possible to delay the onset of AD by tracking the subject's brain network changes and performing interventional therapy in the stage of mild cognitive impairment [9].

One of the essential techniques in brain network analysis is network representation learning, also known as network embedding [5, 10], which aims to embed the subjects' brain networks into meaningful low-dimensional representations. These network representations make it easy to separate damaged or special brain networks from normal controls, thereby providing supplementary or supporting information for traditional clinical evaluations and neuropsychological tests. As one of the most prevalent network representation learning frameworks, graph neural networks (GNNs) [11, 12, 13] take advantage of the excellent representation capability of deep learning [14, 15, 16] and migrate traditional convolution operations from Euclidean space to topological networks with irregular domains [17, 18]. Therefore, many GNN-based embedding methods [8, 19, 20] for brain networks have emerged recently. For brain analysis tasks that treat a subject's brain network as an instance, such as brain disease prediction, GNN-based methods first use stackable network modules to aggregate information from neighbors at different hops. This way, they capture brain networks' structural information and hierarchical patterns. More specifically, GNN learns node-level feature representations by aggregating neighbor information for each node, where the number of GNN layers controls the number of iterative aggregations. Then they apply global pooling on the node-level feature matrices to obtain network-level representations.

Although GNN-based methods have been successfully applied to various brain network analysis tasks, including brain network classification [19] and clustering [5], it is still challenging to release the full potential of GNNs on different brain networks. Specifically, existing works usually utilize GNN with a fixed number of layers to learn all brain network instances, ignoring that different brain networks often require distinct optimal aggregation iterations due to structural differences. On the one hand, more aggregation iterations mean considering neighbors at farther hops, which may prompt some brain networks to learn better representations. Unfortunately, increasing the number of aggregations in GNN may also cause over-smoothing problems [21, 22], which means that all nodes in the same network have indistinguishable or meaningless feature representations. On the other hand, it is infeasible to manually specify the number of iterative aggregations for different brain networks, especially when the instance set is large. A straightforward method to alleviate these problems is to deepen the GNN model with skip-connections (a.k.a., shortcut-connections) [23, 24], which avoid gradient vanishing and a large number of hyperparameter settings. However, this is a sub-optimal strategy because it fails to automate GNN architectures for different brain networks without manual adjustments.

To solve the above problems, in this paper, we propose a novel GNN-based network representation learning framework for brain network analysis, namely BN-GNN. Inspired by the successful application of meta-policy learning [25, 26], we expect a meta-policy that automatically determines the optimal number of feature aggregations (reflected in the number of GNN layers) for a given brain network. Specifically, we model the training process of meta-policy as a Markov decision process (MDP). First of all, we regard the adjacency matrix of a randomly sampled brain network as the initial state and input it into the policy in MDP. Secondly, we guide the construction of the GNN in MDP based on the action (an integer) corresponding to the maximum Q value output by the policy. Here the action value determines the number of GNN layers, which controls the number of feature aggregations on the current brain network. Thirdly, we pool the node features into a network representation. Then we perform network classification to optimize the current GNN and employ a novel strategy to calculate the current immediate reward. Fourthly, we sample the next network instance through a heuristic state transition strategy and record the state-action-reward-state quadruple of this process. In particular, we apply the double deep q-network (DDQN) [27, 28], a classic deep reinforcement learning (DRL) [29] algorithm, to simulate and optimize the policy. Finally, we utilize the trained policy (i.e., meta-policy) as meta-knowledge to guide the construction and training of another GNN and implement specific brain network analysis tasks.

Overall, our main contributions can be summarized as follows:

- A novel network representation learning framework (i.e., BN-GNN) through GNN and DRL is proposed to assist brain network analysis. In this way, we alter the number of feature aggregations for different brain networks, thereby releasing the full potential of traditional GNNs in brain network representation learning.
- To the best of our knowledge, this is the first work that combines GNN with DRL for brain network analysis. We are also the first to use GNNs with different layers to learn different subjects' brain networks.
- Extensive experimental results on eight real-world brain network datasets (i.e., BP-DTI, BP-fMRI, HIV-DTI, HIV-fMRI, ADHD-fMRI, HI-fMRI, GD-fMRI, and HA-EEG) confirm the effectiveness of our proposed BN-GNN over existing state-of-the-art methods in terms of classification accuracy.

The remainder of the paper is organized as follows: Sec. 2 and Sec. 3 describe related work and preliminary knowledge, respectively. Sec. 4 details the implementation of BN-GNN based on graph convolutional network (GCN) [11] and DDQN [28]. Sec. 5 presents the experimental results and corresponding analysis. Sec. 6 concludes the work of this paper.

## 2. Related Work

### 2.1. Graph Neural Networks

Graph neural networks (GNNs) have been widely studied for graph-structured data. GNNs follow the principle that the feature representation of each node is affected by its neighbors in the network. Existing GNNs can be divided into spectral-based or spatial-based methods. One of the most representative GNNs is the graph convolutional network (GCN) [11], which is inspired by the traditional convolutional neural networks (CNNs) on images in the Euclidean space. To improve aggregation performance, the graph attention network (GAT) [12] introduces the attention mechanism to refine the relative importance of neighbors from the perspective of the target node. To improve the aggregation efficiency of large-size graphs, GraphSAGE [13] extracts a fixed number of local neighbors for each target node. In addition, many GNN variants based on the above methods or frameworks have been proposed, and they have made outstanding contributions in network data mining [30, 31], traffic prediction [32, 33], and clinical medicine [8, 34], etc.

### 2.2. Reinforcement Learning Guided Graph Neural Networks

Recently, with the advances of reinforcement learning (RL), many works combine RL with GNNs to further raise the performance boundary of GNNs. For example, [35] proposed a GNN model called CARE-GNN to improve the capability to recognize fraudsters in fraud inspection tasks. CARE-GNN first sorts the neighbors based on their credibility and then uses RL to guide the traditional GNN to filter out the most valuable neighbors for each node to avoid fraudsters from interfering with normal users. [36] proposed a novel recursive and reinforced graph neural network framework learn more discriminative and efficient node representation from multi-relational graph data. [37] proposed a multi-agent reinforced weighted multi-relational GNN framework to learn social message embedding. [38] proposed a graph neural architecture search algorithm, namely GraphNAS. GraphNAS first utilizes a recurrent network to create variable-length strings representing the architectures of GNNs and then applies RL to update the recurrent network for maximizing the expected accuracy of the generated architectures on a validation dataset. [39] proposed a GCN-based algorithm for traffic signal control called NFQI, which applies a model-free RL approach to learn responsive traffic control in order to deal with temporary traffic demand changes when environmental knowledge is insufficient.

Since deep RL (DRL) combines the perception capability of deep learning with the decision capability of RL, it is a new research hotspot in the field of artificial intelligence. For example, [40] proposed a virtual network embedding algorithm (i.e., V3C+GCN) that combines DRL with a GCN-based module. [25] proposed a meta-policy framework (i.e., Policy-GNN), which adaptively learns an aggregation strategy to use DRL to perform various aggregation iterations on different nodes. Though the above methods directly or indirectly use RL or DRL to improve GNNs, there is still no work using DRL to guide GNNs to assist brain network analysis, which often requires different models for different brain networks.

### 2.3. GNN-based Brain Network Representation Learning

Unlike traditional shallow methods for brain network representation learning, such as tensor decomposition [5, 10], some works use GNNs to capture deep feature representations of brain networks for downstream brain analysis tasks. Concretely, [41] proposed a PR-GNN that includes regularized pooling layers, which calculates node pooling scores to infer which brain regions are obligatory parts of certain brain disorders. [42] proposed an aggregator based on an extreme learning machine (ELM) that improves the aggregation ability of graph convolution without iterative adjustment and then offered a model named GNEA for brain network classification based on the aggregator. The Hi-GCN method proposed by [43] performs network representation learning from a hierarchical perspective. While considering the structure of a single brain network and the correlation of subjects in the global population network, Hi-GCN captures the most basic embedding features to improve the classification performance of disease diagnosis. [44] developed an end-to-end graph similarity learning framework for multi-agent brain data analysis, namely HS-GCN, which builds a siamese neural network based on two GCNs and learns brain network representations by means of supervised metrics. [45] proposed a regularized GNN (i.e., RGNN) for emotion recognition based on electroencephalogram. [46] proposed a GCN-based model (i.e., DS-GCNs) to extract efficient disease-related features from functional connectivity matrices that have been widely used in neurological brain disease classification. DS-GCNs calculate a dynamic functional connectivity matrix with a sliding window and implement a long and short-term memory layer based on graph convolution to process dynamic graphs.

In addition to the above-mentioned single-modality brain network research, some GNN-based methods have also been successfully applied to multi-modality brain networks. For example, [8] proposed a deep learning method based on GCN (i.e., MVGCN) for fusing multiple modalities of brain networks in relationship prediction, which helps distinguish Parkinson's

Table 1: Glossary of Notations.

Notation	Definition
$D; D_{train}; D_{val}; D_{test}$	The brain network dataset; The training set of $D$ ; The validation set of $D$ ; The test set of $D$
$G; V; E$	The brain network; The node set of $G$ ; The edge set of $G$
$S; A$	The state space in MDP; The action space in MDP
$\mathbf{W}; \mathbf{A}; \tilde{\mathbf{A}}$	The initial weighted matrix of $G$ ; The adjacency matrix of $G$ ; The normalized form of $\tilde{\mathbf{A}}$
$\tilde{\mathbf{A}}; \mathbf{D}$	The adjacency matrix with self-loop; The degree matrix of $\tilde{\mathbf{A}}$
$\mathbf{E}; \mathbf{F}$	The network-level feature matrix of $D$ ; The node-level feature matrix of $G$
$\mathbf{T}$	The feature transformation matrix or the fully-connected layer
$\mathbf{C}; \hat{\mathbf{C}}$	The importance coefficient matrix of $G$ ; The normalized form of $\mathbf{C}$
$m; n$	The total number of brain networks in $D$ ; The total number of nodes in $V$
$d$	The feature representation dimension of $\mathbf{E}$ or $\mathbf{F}$
$l$	The total number of layers of GNN or the total number of iterative aggregations
$i; j; k$	These notations represent index variables
$s; a; r$	The state in MDP; The action in MDP; The reword in MDP
$t; b$	The total number of timesteps in MDP; The number of all possible actions in $A$
$w$	The window size of the history records in $REW(\cdot)$
$\oplus$	The feature combination operation, such as summation and concatenation
$\pi$	The policy function in MDP or the meta-policy
$\gamma; \epsilon$	The discount coefficient of $\mathcal{R}$ ; The epsilon probability of exploration of $\pi$
$\sigma(\cdot)$	The activation function, such as $Tanh$ and $ReLU$
$AGG(\cdot)$	The feature aggregation function of GNN, such as convolution and attention
$REW(\cdot)$	The immediate reward function in MDP
$PER(\cdot)$	The classification performance metric, such as accuracy.
$\mathcal{R}$	The discounted cumulative return in MDP
$\mathcal{Q}_{eval}; \mathcal{Q}_{target}$	The evaluation DNN in DDQN; The target DNN in DDQN
$\mathcal{L}_{GNN}; \mathcal{L}_{policy}$	The training loss of GNN; The training loss of meta-policy

disease cases from healthy controls. [47] proposed a multi-modality graph normalizer network based on GNNs (i.e., MGN-Net) to normalize and integrate a group of multi-modality brain networks into a single connected network.

Although these GNN-based single- or multi-modality methods have made significant breakthroughs in many brain network analysis tasks, they have failed to implement customized aggregation for different subjects' brain networks in experiments such as brain disease prediction.

### 3. Preliminaries

In this section, we first formulate the brain network analysis problem and then introduce the network representation learning method based on GNN with a fixed number of layers, Markov decision process, and deep reinforcement learning. Table 1 lists necessary notations used throughout the paper.

#### 3.1. Problem Formulation

Generally, a brain network can be represented as a weighted graph  $G = (V, E)$ , where  $V = \{v_1, \dots, v_n\}$  is the set of nodes and  $E \subseteq V \times V$  is the set of weighted edges encoding the interaction between each pair of nodes. Let  $\mathbf{W}$  denote the initial weighted matrix of  $G$  so that  $\mathbf{W}(i, j)$  encodes the relation between  $v_i$  and  $v_j$  if there is an edge and 0 otherwise. Let  $D = \{G_1, \dots, G_m\}$  denote a set of brain networks from  $m$  individual subjects. We assume that brain networks share the same set of nodes but different edges, where a specific region division strategy determines the number of nodes. Given the  $k$ -th brain network  $G_k = (V_k, E_k)$ , we abstract it as a weighted matrix  $\mathbf{W}_k \in \mathbb{R}^{n \times n}$ .

In this paper, we study the problem of brain network representation learning from the perspective of graph-based reinforcement learning, which is used for both classification and clustering. Specifically, we focus on the classification task since it is one of the most important tasks in brain network analysis. Given dataset  $D$ , we assume that the corresponding network labels  $\mathbf{Y}$  are known. For convenience, we denote the training, validation, and test set of  $D$  as  $D_{train}$ ,  $D_{val}$ , and  $D_{test}$ , respectively, where  $D = D_{train} \cup D_{val} \cup D_{test}$ . Based on the brain networks in  $D_{train} \cup D_{val}$ , we first continuously optimize a policy  $\pi$ . Next, we employ the trained policy (i.e., meta-policy) to guide the construction of GNN and utilize the customized GNN to learn the node representations of each brain network that meet the number of feature aggregations. Then, by applying the global pooling at the last layer of GNN, we convert the node-level feature tensor into a low-dimensional network-level representation matrix  $\mathbf{E}$ , allowing brain network instances with different labels to be easily separated. Last, we feed  $\mathbf{E}$  into the full-connected layer to perform brain network classification.

### 3.2. Learning Network Representations with Layer-fixed GNN

GNNs learn node-level feature representations through the network structure. Given a graph  $G = (V, E)$  along with its adjacency matrix  $\mathbf{A} \in \mathbb{R}^{n \times n}$  and initial node feature matrix  $\mathbf{F}^{(0)} \in \mathbb{R}^{n \times d^{(0)}}$ , we express the feature aggregation process of node  $v_i \in V$  in GNN with a fixed number of layers as follows [35]:

$$\mathbf{F}^{(l)}(i) = \sigma \left( \mathbf{F}^{(l-1)}(i) \oplus AGG^{(l)} \left( \{\mathbf{F}^{(l-1)}(j) : \mathbf{A}(i, j) > 0\} \right) \right), \quad (1)$$

where  $\mathbf{F}^{(l-1)} \in \mathbb{R}^{n \times d^{(l-1)}}$  and  $\mathbf{F}^{(l)} \in \mathbb{R}^{n \times d^{(l)}}$  are the input and output of the  $l$ -th layer of GNN.  $AGG^{(l)}$  is the aggregation module at the  $l$ -th layer, and its superscript  $(l)$  means using modules with the same architecture but different parameters to handle each layer.  $\oplus$  is an operation used to combine the features of node  $v_i$  and its neighbors.  $\sigma$  is an activation function, such as *Tanh* and *ReLU*. It is worth noting that  $\mathbf{A}$  should be reliable as it remains unchanged at all layers. Taking graph convolutional network (GCN) [11] with two layers as an example, it implements Eq. 1 through convolution:

$$\begin{aligned} \widehat{\mathbf{A}} &= \widetilde{\mathbf{D}}^{-1/2} \widetilde{\mathbf{A}} \widetilde{\mathbf{D}}^{-1/2} \\ \mathbf{F}^{(2)} &= ReLU(\widehat{\mathbf{A}} ReLU(\widehat{\mathbf{A}} \mathbf{F}^{(0)} \mathbf{T}^{(1)}) \mathbf{T}^{(2)}) \end{aligned} \quad (2)$$

where  $\widehat{\mathbf{A}} \in \mathbb{R}^{n \times n}$  is the symmetrical normalized form of  $\widetilde{\mathbf{A}}$ ,  $\widetilde{\mathbf{A}} = \mathbf{A} + \mathbf{I}$  is the adjacency matrix with self-loop (corresponding to the identity matrix  $\mathbf{I} \in \mathbb{R}^{n \times n}$ ), and  $\widetilde{\mathbf{D}} \in \mathbb{R}^{n \times n}$  is the degree matrix of  $\widetilde{\mathbf{A}}$ . At the first layer, since  $\widehat{\mathbf{A}}$  encodes each node's direct (1-hop) neighbor information,  $\widehat{\mathbf{A}} \mathbf{F}^{(0)}$  essentially implements the first convolution aggregation through summation. At the second layer, the continuous multiplication of the adjacency matrix (i.e.,  $\widehat{\mathbf{A}} ReLU(\widehat{\mathbf{A}})$ ) makes the neighbor's neighbor (2-hop) information included in the second aggregation. Therefore, as the number of layers and aggregation iterations increase, the receptive field of GNN becomes wider, so more neighbors participate in aggregation. In addition,  $\mathbf{T}^{(1)} \in \mathbb{R}^{d^{(0)} \times d^{(1)}}$  and  $\mathbf{T}^{(2)} \in \mathbb{R}^{d^{(1)} \times d^{(2)}}$  are the learnable matrices for feature transformation of the first and second layer, respectively. Unlike GCN, which equally distributes the importance of all neighbors, graph attention network (GAT) [12] uses the attention mechanism to assign different weights to different neighbors when summing neighbor features. Taking the first layer of a single-head GAT as an example, the node feature aggregation process can be expressed as follow:

$$\begin{aligned} \mathbf{C}(i, j) &= (\mathbf{F}^{(0)}(i) \mathbf{T}^{(1)} \oplus \mathbf{F}^{(0)}(j) \mathbf{T}^{(1)}) q^T \\ \widehat{\mathbf{C}} &= softmax(\mathbf{C}(i, j)) = \frac{exp(ReLU(\mathbf{C}(i, j)))}{\sum_{v_k \in V(i)} exp(ReLU(\mathbf{C}(i, k)))}, \\ \mathbf{F}^{(1)}(i) &= ReLU \left( \sum_{v_j \in V(i)} \widehat{\mathbf{C}} \mathbf{F}^{(0)}(j) \mathbf{T}^{(1)} \right) \end{aligned} \quad (3)$$

where  $\mathbf{F}^{(0)}(i) \in \mathbb{R}^{1 \times d^{(0)}}$  represents the initial feature representation of node  $v_i$ ,  $\mathbf{T}^{(1)} \in \mathbb{R}^{d^{(0)} \times d^{(1)}}$  is the feature transformation matrix whose parameters are shared,  $\oplus$  is the concatenation operation, and  $q \in \mathbb{R}^{1 \times 2d^{(1)}}$  is the attention feature vector.  $\mathbf{C}(i, j)$  is the importance coefficient (a real number) of node  $v_j$  to node  $v_i$ ,  $\widehat{\mathbf{C}}$  is the normalized form of  $\mathbf{C}$ , and  $\mathbf{F}^{(1)}(i) \in \mathbb{R}^{1 \times d^{(1)}}$  is the updated feature representation of the target node  $v_i$ . Here  $V(i) = \{v_j : \mathbf{A}(i, j) > 0\}$  indicates the neighbor set of node  $v_i$ . Similarly, GAT also controls the number of feature aggregations by changing the number of layers. After the final aggregation is completed at the last layer  $l$ , GNN-based methods perform global pooling on all nodes to obtain the final network representation. The process of global average pooling is described as follows:

$$\mathbf{E}(i) = \frac{1}{n} \sum_{v_j \in V} \mathbf{F}_i^{(l)}(j), \quad (4)$$

where  $\mathbf{E}(i) \in \mathbb{R}^{1 \times d^{(l)}}$  and  $\mathbf{F}_i^{(l)}(j)$  are the network-level feature vector and node-level feature matrix of the  $i$ -th network instance  $G_i$ , respectively. Then the cross entropy loss of this part can be calculated as follows:

$$\mathcal{L}_{GNN} = - \sum_{G_i \in D_{train}} \log(\mathbf{E}(i) \mathbf{T}^{(l+1)} \mathbf{Y}(i)^T), \quad (5)$$

where  $\mathbf{T}^{(l+1)}$  is the fully connected layer used as the classifier, and  $\mathbf{Y}(i)$  corresponds to the label of the  $i$ -th brain network.

In brain network analysis, most brain networks can be abstracted as weighted matrices describing the connections among brain regions, but they often do not have initial node features. How to design information node features and corresponding edge weights for GNN learning is still rarely explored. A common strategy is to use the initial weighted matrix  $\mathbf{W}$  associated with each brain network  $G$  as its initial node features (i.e.,  $\mathbf{F}^{(0)} = \mathbf{W}$ ) and define a group-level adjacency matrix  $\mathbf{A}$  for GNN. For example, [8] defined  $\mathbf{A}$  as a k-nearest neighbor (KNN) graph based on the coordinate information, and [48] introduced a random generated graph Laplacian using the small-world model to infer  $\mathbf{A}$  during the GNN training. However, using the same adjacency matrix for different brain networks may blur the differences between different networks. Different from the previous work [8, 48], our goal is to generate a separate adjacency matrix for each brain network and implement network representation learning for different brain networks based on GNNs with different layers.

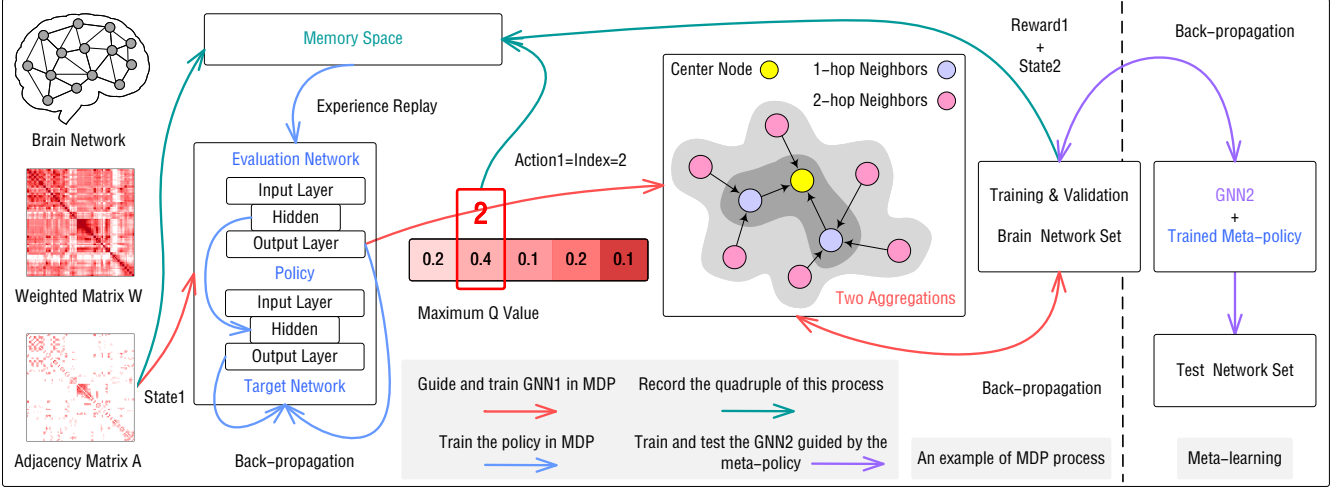


Figure 1: Overview of our proposed framework BN-GNN for brain network representation learning. The left side of the dotted line illustrates an example of the MDP process. We first use the adjacency matrix generated by the network building module as the current state and input it into the policy. Then we select the current action according to the maximum Q value output by the policy. Here we treat the index of the selected action in the action space as the action value to guide the number of aggregations of the current brain network in GNN. After feature aggregation, we apply pooling to obtain the network representation and train the GNN model in MDP. Subsequently, the current reward is calculated by comparing the performance changes on the verification set. Finally, the next state is obtained according to the state transition strategy. To train the policy in MDP, we record the state-action-reward-state quadruple of this process to the memory space and follow the DDQN method to calculate the loss of the policy. On the right side of the dotted line, we apply the trained meta-policy to guide the training of a new GNN and perform brain network analysis tasks.

### 3.3. Markov Decision Process

Markov decision process (MDP) is a mathematical model of sequential decision, used to simulate the random actions and rewards that the agent can achieve in an environment with Markov properties. Here we denote the MDP as a quintuple  $(S, A, \pi, REW, \mathcal{R})$ , where  $S$  is the set of all states (a.k.a., state space),  $A$  is the set of all possible actions (a.k.a., action space),  $\pi$  is the policy that outputs the conditional probability distribution of actions for a given state,  $REW : S \times A \rightarrow \mathbb{R}$  is the immediate reward function, and  $\mathcal{R}$  is the accumulation of rewards over time (a.k.a, return). The decision process in each timestep  $i \in [1, t]$  is as follows: the agent first perceives the current state  $s_i \in S$  and performs an action  $a_i \in A$  according to the policy  $\pi$ . Then, the environment (which is affected by the action  $a_i$ ) feeds back to the agent the next state  $s_{i+1}$  as well as a reward  $r_i = REW(s_i, a_i)$ . In the standard MDP, our goal is to train the policy  $\pi$  to maximize the discounted cumulative return. The calculation process of the return is described as follows:

$$\mathcal{R} = r_1 + \gamma r_2 + \gamma^2 r_3 + \cdots + \gamma^{t-1} r_t = \sum_{i=1}^t \gamma^{i-1} r_i, \quad (6)$$

where  $\gamma \in (0, 1)$  is the discount coefficient used to constrain rewards with lower reliability in the future. In the following subsection, we present the training details of the policy  $\pi$ .

### 3.4. Solving MDP with Deep Reinforcement Learning

In many scenarios, the state space  $S$  is huge or inexhaustible. In this case, it is sub-optimal or infeasible to train the policy  $\pi$  by maintaining and updating a state-action table. Deep reinforcement learning (DRL) [29] is an effective solution because it can use neural networks to simulate and approximate the actual relationship between any state and all possible actions. Here, we focus on a classic DRL algorithm called double deep q-learning (DDQN) [27, 28], which uses two deep neural networks (DNNs) to simulate the policy  $\pi$ . Concretely, in each timestep  $i$ , DDQN first inputs the current state  $s_i$  into the evaluation DNN to obtain the predicted Q values of all actions and regard the action corresponding to the maximum Q value as the current action, which should conform to the following formula:

$$a_i = \begin{cases} \text{random action,} & \text{w.p. } \epsilon \\ \text{argmax}_{a_i}(Q_{eval}(s_i, a_i)), & \text{w.p. } 1 - \epsilon \end{cases}, \quad (7)$$

where  $\epsilon$ -greedy is used to enhance the generalization ability of DDQN and avoid the dilemma of exploration and utilization. The maximum Q value  $\max_{a_i}(Q(s_i, a_i))$  is essentially the expected maximum discounted return in the current state  $s_i$ , and the corresponding Bellman equation can be expressed as follows:

$$\begin{aligned} \max_{a_i}(Q_{eval}(s_i, a_i)) &= \max(\mathcal{R}_i) = \max(r_i + \gamma(r_{i+1} + \gamma(r_{i+2} + \dots))) \\ &= r_i + \gamma \max(\mathcal{R}_{i+1}). \end{aligned} \quad (8)$$

After determining the current action  $a_i$ , DDQN uses the reward function (designed according to the specific environment) to calculate the current actual reward (i.e.,  $r_i = REW(s_i, a_i)$ ) and then performs state transition to obtain the next state  $s_{i+1}$ . Moreover, there is a memory space in DDQN that records each MDP process (also known as “experience” and recorded as a state-action-reward-state quadruple  $\langle s_i, a_i, r_i, s_{i+1} \rangle$ ). To optimize DNNs with experience replay, DDQN first records the current experience and then randomly extracts a memory block from the memory space. For example, through the experience  $\langle s_i, a_i, r_i, s_{i+1} \rangle$ , the loss of DNNs (i.e., policy) can be calculated as follows:

$$\begin{aligned} \mathcal{L}_{policy} &= (\max(Q_{target}(s_i, a_i)) - \max(Q_{eval}(s_i, a_i)))^2 \\ &= (r_i + \gamma \max_{a_{i+1}}(Q_{target}(s_{i+1}, a_{i+1})) - \max_{a_i}(Q_{eval}(s_i, a_i)))^2, \end{aligned} \quad (9)$$

where state  $s_i$  is input to the evaluation DNN to obtain the predicted maximum Q value  $\max_{a_i}(Q_{eval}(s_i, a_i))$  in the  $i$ -th timestep, the next state  $s_{i+1}$  is input to the target DNN to calculate the maximum Q value  $\max_{a_{i+1}}(Q_{target}(s_{i+1}, a_{i+1}))$  in the next timestep, and  $r_i$  is the actual reward. Based on the Bellman equation, DDQN takes the  $\max(Q_{target}(s_i, a_i))$  output from the target DNN as the actual maximum Q value in timestep  $i$  and trains the evaluation DNN through the back-propagation algorithm. It is worth noting that DDQN does not update the target network through loss but copies the parameters of the evaluation DNN to the target DNN. In this way, DDQN effectively alleviates the over-estimation problem often found in DRL. Since DDQN uses two DNNs to simulate the policy  $\pi$ , the above is also the training process of  $\pi$ .

## 4. Methodology

Fig. 1 presents an overview of our proposed brain network representation learning framework BN-GNN, which consists of three modules: network building module, meta-policy module and GNN module. The network building module provides the state space for the meta-policy module. The meta-policy module uses the feedback (i.e., rewards) of the GNN module to search for the optimal meta-policy  $\pi$  continuously, and the GNN module performs brain network representation learning according to the guidance (i.e., actions) of the meta-policy. Next, we introduce the technical details of each module.

### 4.1. Network Building Module

The network building module generates adjacency matrices from the brain networks’ initial weighted matrices, providing state space for the meta-policy module. In GNN, an essential module is the feature aggregation based on the adjacency matrix  $\mathbf{A}$ . Therefore, the adjacency matrix should be appropriately designed to reflect the neighborhood correlations because it directly affects the node feature representation learning. Inspired by the previous work in [8], we utilize the k-nearest neighbor (KNN) to construct reliable adjacency matrices to facilitate learning brain network representation for GNNs. Specifically, given the brain network  $G = (V, E)$ , we utilize its weighted matrix  $\mathbf{W} = \mathbf{F}^{(0)}$  and KNN to obtain reliable neighbors  $V(i)$  of any node  $v_i \in V$ . If  $v_i \in V(j)$  or  $v_j \in V(i)$ , then  $\mathbf{A}(i, j) = 1$  and  $\mathbf{A}(j, i) = 1$ , otherwise  $\mathbf{A}(i, j) = 0$  and  $\mathbf{A}(j, i) = 0$ . After that, we calculate new edge confidences to refine the reliable adjacency matrix  $\mathbf{A}$  as follows:

$$\mathbf{A}(i, j) = \begin{cases} \exp(-\|\mathbf{F}^{(0)}(i) - \mathbf{F}^{(0)}(j)\|), & \mathbf{A}(i, j) = 1 \\ 0, & \mathbf{A}(i, j) = 0 \end{cases}, \quad (10)$$

where  $\mathbf{F}^{(0)}(i)$  is the  $i$ -th row of  $\mathbf{F}^{(0)}$  and the initial feature vector of node  $v_i$ . It is worth noting that this module is also used to construct the subject network in the state transition strategy, which will be introduced in the following subsection.

### 4.2. Meta-policy Module

The meta-policy module trains a policy that can be viewed as meta-knowledge to determine the number of aggregations of brain network features in GNN. As mentioned in Sec. 3.3, we model the training process of the policy  $\pi$  as a Markov decision process (MDP) that contains five essential components, i.e.,  $(S, A, \pi, REW, \mathcal{R})$ . Here, we give the relevant definitions in the context of brain network embedding in timestep  $i$ .

- State space ( $S$ ): The state  $s_i \in S$  represents the adjacency matrix of the brain network.
- Action space ( $A$ ): The action  $a_i \in A$  determines the number of iterations for feature aggregation that the brain network requires, which is reflected in the number of GNN layers. Considering that the number of GNN layers is a positive integer, we define the index of each action in the action space as the corresponding action value.

---

**Algorithm 1 BN-GNN: GNN-based brain network representation learning framework**


---

**Input:** Brain network dataset  $D$ , number of timesteps  $t$ , number of all possible actions  $b$ , discount coefficient  $\gamma$ , epsilon probability  $\epsilon$ , window size of the history records  $w$ .

- 1: Generate adjacency matrices of brain networks and the subject network via Eq. (10),  $\mathbf{A}(i, j) = \exp(-\|\mathbf{F}^{(0)}(i) - \mathbf{F}^{(0)}(j)\|)$  or 0.
- 2: Initialize two DNNs in DDQN and two GNNs with  $b$  layers.
- 3: Randomly sample a brain network from  $D_{train}$  and get the starting state according to the adjacency matrix.
- 4: **for**  $i = 1, 2, \dots, t$  **do**
- 5:     Select the action via Eq. (7),  $a_i = \text{argmax}_{a_i}(Q_{eval}(s_i, a_i))$  or a random action.
- 6:     Train the action value guided GNN1 in MDP via Eq. (5),  $\mathcal{L}_{GNN} = -\sum_{G_i \in D_{train}} \log(\mathbf{E}(i)\mathbf{T}^{(i+1)})\mathbf{Y}(i)^T$ .
- 7:     Calculate the reward via Eq. (12),  $r_i = REW(s_i, a_i) = PER(s_i, a_i) - \frac{1}{w} \sum_{i-w}^{i-1} PER(s_i, a_i)$ .
- 8:     Sample the next state and record this process.
- 9:     Train the policy in MDP via Eq. (9),  $\mathcal{L}_{policy} = (\max(Q_{target}(s_i, a_i)) - \max(Q_{eval}(s_i, a_i)))^2$ .
- 10: **end for**
- 11: Use the trained policy, meta-policy as meta-knowledge to guide the training and testing of GNN2.
- 12: Obtain network representations of the test set  $D_{test}$  and perform brain analysis tasks.

---

• Policy ( $\pi$ ): The policy in timestep  $i$  outputs action  $a_i$  according to the input state  $s_i$ . Here we apply double deep q-network (DDQN) presented in Sec. 3.4 to simulate and train the policy and call the trained policy a meta-policy.

• Reward function ( $REW$ ): The reward function outputs the reward  $r_i$  in timestep  $i$ . Since we expect to improve network representation performance through policy-guided aggregations, we intuitively define the current immediate reward  $r_i$  as the difference (a decimal) between the current validation classification performance and the performance of the previous timestep.

• Return ( $\mathcal{R}$ ): The return  $\mathcal{R}_i$  in timestep  $i$  indicates the discounted accumulation of all rewards in the interval  $[i, t]$ . Based on the DDQN, we approximate the Q values output by the DNNs in the DDQN to the rewards over different actions. Since DDQN always chooses the action that maximizes return, it aligns with the goal of standard MDP.

According to these definitions, the process of the meta-policy module in each timestep  $i$  includes five stages: 1) Sample a brain network and take its adjacency matrix as the current state  $s_i$ . 2) Determine the number of layers of the GNN that processes the current brain network according to the action  $a_i$  corresponding to the maximum Q value output by the policy  $\pi$ . 3) Calculate the current reward  $r_i$  based on performance changes (technical details will be introduced in the following subsection). 4) Obtain the next state  $s_{i+1}$  with a new heuristic strategy for state transition. Concretely, we abstract the brain network of each subject as a coarse node and construct a subject network according to the network building module, where the initial node features are obtained by vectorizing the weighted matrices. Then we realize state transition through node sampling. For example, given the current state  $s_i$  and action  $a_i$ , we randomly sample a  $a_i$ -hop neighbor of the coarse node corresponding to state  $s_i$  in the subject's network, where the adjacency matrix of the brain network corresponding to the sampled neighbor is the next state  $s_{i+1}$ . In this way, the state transition obeys Markov, i.e., the next state  $s_{i+1}$  is only affected by the current state  $s_i$  without considering the previous states. 5) Record the process of this timestep and train the policy  $\pi$  according to Eq. 9 and the back-propagation algorithm.

#### 4.3. GNN Module

The GNN module contains two GNNs with a pooling layer to learn brain network representations. The first GNN (called GNN1) is used in the MDP to train the policy  $\pi$ . As defined in Sec. 4.2, each action is a positive integer in the interval  $[1, b]$ , where  $b$  is the total number of all possible actions. Since the action  $a_i$  specifies the number of feature aggregations and GNN achieves different aggregations by controlling the number of layers, GNN1 needs to stack  $j$  neural networks when  $a_i = j$  ( $j$  is the index of  $a_i$  in  $A$ ). Considering that the actions in different processes are usually different, reconstructing GNN1 in each timestep is very time- and space-consuming. To alleviate this problem, we use a parameter sharing mechanism to construct a  $b$ -layer GNN1. For example, given the current action  $a_i = j$ , we only use the first  $j$  layers of GNN1 to learn the current brain network  $G_i$ . The aggregation process realized by graph convolutional network (GCN) [11] is as follows:

$$\mathbf{F}^{(j)} = \text{ReLU}(\widehat{\mathbf{A}} \cdots \text{ReLU}(\widehat{\mathbf{A}}\mathbf{F}^{(0)}\mathbf{T}^{(1)}) \cdots \mathbf{T}^{(j)}). \quad (11)$$

After obtaining the final node feature matrix  $\mathbf{F}^{(j)}$ , we apply the pooling of Eq. (4) to obtain the network representation. Then we use the back-propagation algorithm of Eq. (5) to train GNN1. Since the current timestep only involves the first  $b$  layers of GNN1, only the parameters of the first  $b$  layers are updated. Compared with constructing a GNN for each network separately in each timestep, the parameter sharing mechanism significantly improves the training efficiency.

To calculate the current reward  $r_i$ , we measure the classification performance of GNN1 on the validation set  $D_{val}$ . The immediate reward function in the MDP is defined as follows:

$$r_i = REW(s_i, a_i) = PER(s_i, a_i) - \frac{1}{w} \sum_{i-w}^{i-1} PER(s_i, a_i), \quad (12)$$

Table 2: Statistics of Brain Network Datasets.

Dataset	BP-DTI	BP-fMRI	HIV-DTI	HIV-fMRI	ADHD-fMRI	HI-fMRI	GD-fMRI	HA-EEG
Network Instances	70	70	97	97	83	79	85	61
Healthy/Male/Active	35	35	45	45	46	44	36	21
Patient/Female/Passive	35	35	52	52	37	35	49	40
Nodes $\times$ Nodes	82 $\times$ 82	82 $\times$ 82	90 $\times$ 90	90 $\times$ 90	200 $\times$ 200	200 $\times$ 200	200 $\times$ 200	68 $\times$ 68

where  $PER$  represents the performance metric of the classification result on the validation data (here we apply accuracy).  $w$  indicates the number of historical records used to determine benchmark performance  $\frac{1}{w} \sum_{i-w}^{i-1} PER(s_i, a_i)$ . Compared with only considering the performance of the previous timestep ( $i - 1$ ), the benchmark based on multiple historical performances improves the reliability of  $r_i$ .

Since the training of GNN1 and policy in MDP are usually not completed in the same timestep, it is inconvenient and inappropriate to use GNN1 to perform brain analysis tasks on the test set  $D_{test}$ . Therefore, after MDP, we apply the trained meta-policy to guide the training and testing of a new GNN (called GNN2), where GNN2 and GNN1 have the same aggregation type and parameter sharing mechanism. The detailed algorithm of BN-GNN is presented in Algorithm 1.

## 5. Experiments

In this section, eight real-world brain network datasets are used to evaluate our proposed BN-GNN. We first introduce the datasets used in the experiments (Sec. 5.1), the comparison baselines, and the experimental settings (Sec. 5.2). We then conduct sufficient experiments on the brain network classification task to answer the following three research questions (RQs) about the effectiveness of our BN-GNN:

- RQ1. How does BN-GNN perform compared to other state-of-the-art brain network representation methods? (Sec. 5.3)
- RQ2. Can the three modules included in BN-GNN improve brain network representations learning? (Sec. 5.4)
- RQ3. How do important hyperparameters in BN-GNN affect model representation performance? (Sec. 5.5)

### 5.1. Datasets

Eight brain network datasets covering different neurological disorders are used for evaluation. Table 2 shows the statistics of all datasets. More details of these datasets are described as follows:

**Human Immunodeficiency Virus Infection (HIV-DTI & HIV-fMRI):** This dataset is collected from Chicago Early HIV Infection Study at Northwestern University [49] using two modalities, i.e., diffusion tensor imaging (DTI) and functional magnetic resonance imaging (fMRI). We randomly select 35 HIV patients and 35 healthy controls, where there is no difference in gender, age, education level, etc. between the two groups. Similar to the data preprocessing process proposed in [50], we process the HIV data according to the following steps: First, the fMRI data is processed by the DPARSF [51]. It realigns all brain images to the first volume, performs slice time correction and normalizes them to standard MNI templates. Then, we utilize a Gaussian kernel (8-mm) to smooth these normalized brain images. And we also perform linear trend and band-pass filtering (0.01-0.08 Hz) to eliminate the effects of high-frequency noise and low-frequency drift. After that, for each brain, the gray matter is divided into 116 anatomical volumes of interest through the automatic anatomical labeling atlas [52], where each atlas represents a specific brain region. Finally, by eliminating 26 cerebellar regions and calculating the correlation coefficients among the remaining 90 brain regions, we obtain the initial weighted matrices of the brain networks of all subjects. Similarly, we first use the FSL [53], containing distortion correction, noise filtering, and repetitive sampling from the distributions of principal diffusion directions for each voxel to process the DTI data. Then we obtain the corresponding weighted matrices of brain networks with 90 regions.

**Bipolar Disorder (BP-DTI & BP-fMRI):** This dataset also contains fMRI and DTI modalities, including 52 patients with bipolar disorder and 45 age- and gender-matched healthy controls [54]. For the fMRI data, we employ the CONN toolbox [55] to get the initial brain networks. Concretely, we first realign and co-register the original EPI images and then perform normalization and smoothing. After that, the confound effects from motion artifacts, white matter, and cerebrospinal fluid will disappear. Finally, the initial brain networks are derived using the pairwise signal correlations based on the 82 labeled cortical gray matter regions. For the DTI data, we follow the data processing strategy in [50] to generate brain networks whose regions are the same as those of the fMRI network.

**Attention Deficit Hyperactivity Disorder (ADHD-fMRI) & Hyperactive Impulsive Disorder (HI-fMRI) & Gender (GD-fMRI):** The initial data was constructed from the whole brain fMRI atlas [56]. Following the work in [57], we use the functional segmentation result CC200 from [56], which divides each brain into 200 regions of interest (ROIs). In order to explore the relationship between ROIs, we record the average value of each ROI in a specific voxel time course. Similarly, we obtain the correlation between the two ROIs according to the Pearson correlation between the two time courses, and generate

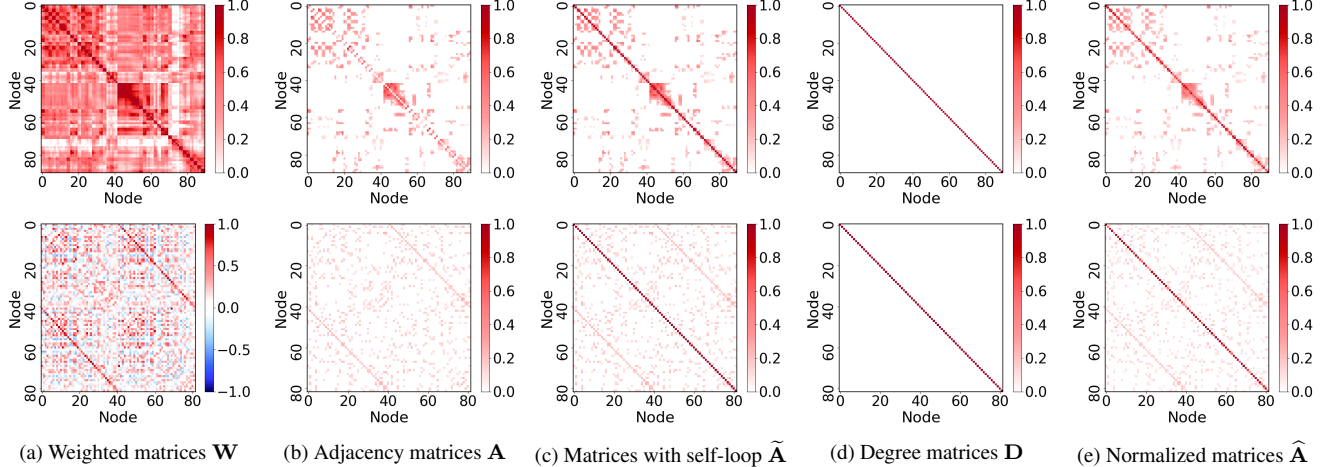


Figure 2: Examples of brain networks of two subjects in fMRI modality. The subject above is from HIV, while below one is from BP. From left to right are the initial weighted matrices  $\mathbf{W}$ , the adjacency matrices  $\mathbf{A}$  generated by the network building module (Eq. 10), and the other matrices involved in the GCN aggregation process (Eq. 2).

three reliable brain network instance sets based on the threshold specified in the work [57]. More details on data collection and processing are available in [56, 57].

**Hearing Activity (HA-EEG):** The raw electroencephalogram (EEG) data was recorded from 61 healthy adults using 62 electrodes [58]. The participants were either actively listening to individual words over headphones (active condition) or watching a silent video and ignoring the speech (passive condition). To transform the dataset into a usable version, we perform source analysis using the fieldtrip toolkit [59] with a cortical-sheet based source model and a boundary element head model. Specifically, we calculate the coherence of all sources and segment the sources based on the 68 regions of the Desikan-Killiany cortical atlas. Furthermore, we utilize the imaginary part of the coherence spectrum as the connectivity metric to reduce the effect of electric field spread [60].

## 5.2. Baselines and Settings

To evaluate our BN-GNN, we compare it with other state-of-the-art baselines. All baselines are summarized as follows:

**DeepWalk & Node2Vec** [61, 62]: The main idea of Deepwalk is to perform random walks in the network, then generate a large number of node sequences, further input these node sequences as samples into word2vec [63], and finally obtain low-dimensional node representations. Compared with DeepWalk, Node2Vec balances the homophily and structural equivalence of the network through biased random walks. Both of them are commonly used baselines in network representation learning.

**GCN & GAT** [11, 12]: Graph convolutional network (GCN) performs convolution aggregations in the graph Fourier domain, while graph attention network (GAT) performs aggregations in combination with the attention mechanism. Both of them are state-of-the-art GNN algorithms.

**GCN+skip & GAT+skip:** Following the work in [24], we construct GCN+skip and GAT+skip by adding residual skip-connections to GCN and GAT, respectively.

**GraphSAGE & FastGCN** [13, 64]: They are two improved GNN algorithms with different sampling strategies. For the sake of computational efficiency, GraphSAGE only samples a fixed number of neighbor nodes for each node as the objects to be aggregated. Unlike GraphSAGE sampling neighbor nodes, FastGCN samples all nodes to construct a new topology based on the original network, and then capture the global information of the network.

**PR-GNN & GNEA & Hi-GCN** [41, 42, 43]: Three GNN-based baselines for brain network analysis, all of which contain methods for optimizing the initial brain network generated by neuroimaging technology. PR-GNN utilizes the regularized pooling layers to filter nodes in the network and uses GAT for feature aggregation. GNEA selects a fixed number of neighbors for all nodes based on the correlation coefficient in each brain network. Hi-GCN uses the eigenvector-based pooling layers EigenPooling to generate multiple coarse-grained sub-graphs from the initial network and then aggregates network information hierarchically and generates network representations.

**SDBN** [65]: This is a brain network representation learning model based on convolutional neural networks (CNNs) [66].

In the experiments, we implement our framework using GCN and GAT, respectively, namely **BN-GCN and BN-GAT**. Moreover, we set the total number of timesteps  $t$  to 1000, the total number of all possible actions  $b$  to 3, the window size  $w$  of  $REW$  to 20, and the discount coefficient  $\gamma$  to 0.95. For the epsilon probability  $\epsilon$ , we set it to decrease linearly in the first 20 timesteps, with a starting probability of 1.0 and an ending probability of 0.05. For all GNN-based methods, we use  $ReLU$

Table 3: Comparison of the average accuracy of different methods on brain network classification tasks. The first part compares the experimental results of multiple methods, while the second and third parts refine the representation performance of GCNs and GATs with different layers. The bold and italicized values in each part represent the best and second-best results of all methods, respectively.  $\uparrow$  indicates the improvement (%) of our BN-GNN compared to the best baseline of each part

Method	Layers	BP-DTI	BP-fMRI	HIV-DTI	HIV-fMRI	ADHD-fMRI	HI-fMRI	GD-fMRI	HA-EEG
DeepWalk	-	0.520 $\pm$ 0.097	0.530 $\pm$ 0.134	0.514 $\pm$ 0.159	0.485 $\pm$ 0.130	0.512 $\pm$ 0.141	0.462 $\pm$ 0.148	0.550 $\pm$ 0.127	0.566 $\pm$ 0.270
Node2Vec	-	0.530 $\pm$ 0.110	0.550 $\pm$ 0.111	0.514 $\pm$ 0.145	0.500 $\pm$ 0.172	0.525 $\pm$ 0.075	0.475 $\pm$ 0.122	0.562 $\pm$ 0.170	0.583 $\pm$ 0.200
PR-GNN	2	0.590 $\pm$ 0.186	0.630 $\pm$ 0.110	0.557 $\pm$ 0.174	0.585 $\pm$ 0.100	0.625 $\pm$ 0.167	0.600 $\pm$ 0.165	0.600 $\pm$ 0.145	0.650 $\pm$ 0.157
GNEA	3	0.560 $\pm$ 0.149	0.600 $\pm$ 0.134	0.557 $\pm$ 0.118	0.585 $\pm$ 0.196	0.550 $\pm$ 0.127	0.562 $\pm$ 0.160	0.612 $\pm$ 0.087	0.633 $\pm$ 0.221
HI-GCN	3	0.540 $\pm$ 0.162	0.600 $\pm$ 0.109	0.528 $\pm$ 0.192	0.571 $\pm$ 0.127	0.562 $\pm$ 0.128	0.562 $\pm$ 0.160	0.587 $\pm$ 0.148	0.616 $\pm$ 0.183
GraphSAGE	2	0.610 $\pm$ 0.192	0.610 $\pm$ 0.113	0.571 $\pm$ 0.202	0.600 $\pm$ 0.124	0.575 $\pm$ 0.127	0.575 $\pm$ 0.100	0.600 $\pm$ 0.165	0.716 $\pm$ 0.076
FastGCN	2	0.590 $\pm$ 0.113	0.620 $\pm$ 0.140	0.585 $\pm$ 0.134	0.628 $\pm$ 0.145	0.612 $\pm$ 0.180	0.600 $\pm$ 0.145	0.600 $\pm$ 0.175	0.700 $\pm$ 0.194
BN-GNN	1~3	<b>0.630<math>\pm</math>0.167</b>	<b>0.640<math>\pm</math>0.120</b>	<b>0.614<math>\pm</math>0.111</b>	<b>0.642<math>\pm</math>0.146</b>	<b>0.637<math>\pm</math>0.130</b>	<b>0.612<math>\pm</math>0.205</b>	<b>0.637<math>\pm</math>0.141</b>	<b>0.733<math>\pm</math>0.200</b>
Gain	-	<b>2.0<math>\uparrow</math></b>	<b>1.0<math>\uparrow</math></b>	<b>2.9<math>\uparrow</math></b>	<b>1.4<math>\uparrow</math></b>	<b>1.2<math>\uparrow</math></b>	<b>1.2<math>\uparrow</math></b>	<b>2.5<math>\uparrow</math></b>	<b>1.7<math>\uparrow</math></b>
GCN	1	0.560 $\pm$ 0.101	0.600 $\pm$ 0.148	0.542 $\pm$ 0.178	0.557 $\pm$ 0.174	0.562 $\pm$ 0.150	0.587 $\pm$ 0.080	0.600 $\pm$ 0.122	0.650 $\pm$ 0.189
GCN	2	0.590 $\pm$ 0.130	0.610 $\pm$ 0.122	0.571 $\pm$ 0.180	0.600 $\pm$ 0.166	0.600 $\pm$ 0.165	0.587 $\pm$ 0.125	0.600 $\pm$ 0.108	0.666 $\pm$ 0.129
GCN	3	0.540 $\pm$ 0.180	0.600 $\pm$ 0.184	0.542 $\pm$ 0.189	0.585 $\pm$ 0.118	0.525 $\pm$ 0.122	0.562 $\pm$ 0.187	0.575 $\pm$ 0.150	0.616 $\pm$ 0.106
GCN+skip	3	0.590 $\pm$ 0.164	0.620 $\pm$ 0.116	0.585 $\pm$ 0.134	0.528 $\pm$ 0.111	0.562 $\pm$ 0.170	0.575 $\pm$ 0.160	0.600 $\pm$ 0.183	0.700 $\pm$ 0.163
BN-GCN	1~3	<b>0.610<math>\pm</math>0.170</b>	<b>0.640<math>\pm</math>0.120</b>	<b>0.614<math>\pm</math>0.111</b>	<b>0.642<math>\pm</math>0.172</b>	<b>0.637<math>\pm</math>0.130</b>	<b>0.600<math>\pm</math>0.165</b>	<b>0.625<math>\pm</math>0.125</b>	<b>0.716<math>\pm</math>0.197</b>
Gain	-	<b>2.0<math>\uparrow</math></b>	<b>2.0<math>\uparrow</math></b>	<b>2.9<math>\uparrow</math></b>	<b>4.2<math>\uparrow</math></b>	<b>3.7<math>\uparrow</math></b>	<b>1.3<math>\uparrow</math></b>	<b>2.5<math>\uparrow</math></b>	<b>1.6<math>\uparrow</math></b>
GAT	1	0.570 $\pm$ 0.141	0.620 $\pm$ 0.172	0.542 $\pm$ 0.261	0.571 $\pm$ 0.169	0.562 $\pm$ 0.128	0.575 $\pm$ 0.203	0.612 $\pm$ 0.189	0.650 $\pm$ 0.203
GAT	2	0.590 $\pm$ 0.130	0.610 $\pm$ 0.157	0.585 $\pm$ 0.149	0.614 $\pm$ 0.111	0.600 $\pm$ 0.215	0.587 $\pm$ 0.137	0.612 $\pm$ 0.152	0.683 $\pm$ 0.174
GAT	3	0.550 $\pm$ 0.128	0.610 $\pm$ 0.144	0.571 $\pm$ 0.202	0.585 $\pm$ 0.149	0.550 $\pm$ 0.127	0.575 $\pm$ 0.160	0.612 $\pm$ 0.171	0.666 $\pm$ 0.235
GAT+skip	3	0.600 $\pm$ 0.184	0.610 $\pm$ 0.083	0.600 $\pm$ 0.153	0.557 $\pm$ 0.162	0.575 $\pm$ 0.169	0.587 $\pm$ 0.185	0.625 $\pm$ 0.111	0.700 $\pm$ 0.124
BN-GAT	1~3	<b>0.630<math>\pm</math>0.167</b>	<b>0.640<math>\pm</math>0.128</b>	<b>0.614<math>\pm</math>0.181</b>	<b>0.642<math>\pm</math>0.146</b>	<b>0.612<math>\pm</math>0.180</b>	<b>0.612<math>\pm</math>0.205</b>	<b>0.637<math>\pm</math>0.141</b>	<b>0.733<math>\pm</math>0.200</b>
Gain	-	<b>3.0<math>\uparrow</math></b>	<b>2.0<math>\uparrow</math></b>	<b>1.4<math>\uparrow</math></b>	<b>2.8<math>\uparrow</math></b>	<b>1.2<math>\uparrow</math></b>	<b>2.5<math>\uparrow</math></b>	<b>1.2<math>\uparrow</math></b>	<b>3.3<math>\uparrow</math></b>

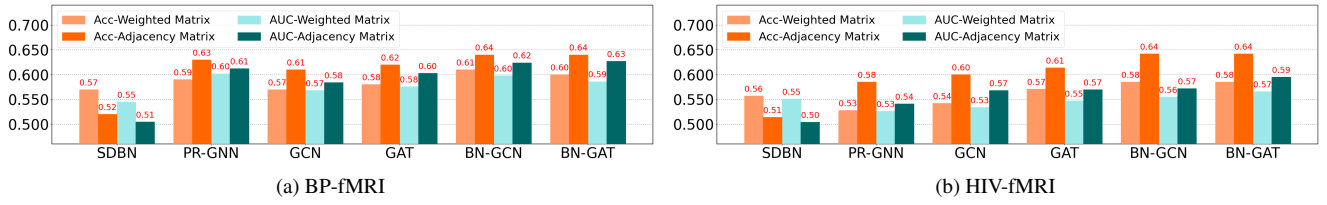


Figure 3: Visualization of ablation experiments to verify the performance of the network building module on the two datasets.

with a slope of 0.2 as the activation function of each feature aggregation layer and use a dropout mechanism with a dropout rate of 0.3 between every two adjacency neural networks. For a fair comparison, we use *Adam* optimizers with learning rates of 0.0005 and 0.005 to train the policy and GNN2, respectively. We set the network representation dimension of all methods to 128 and employ the strategies mentioned in the corresponding papers to adjust the parameters of all baselines and report their performance with the best settings. Besides, we use the same data split ( $|D_{train}| : |D_{val}| : |D_{test}| = 8 : 1 : 1$ ) to repeat each experiment 10 times, where each experiment records the test result with the highest verification value within 100 epochs. All experiments are performed on the same server with two 20-core CPUs (126G) and an NVIDIA Tesla P100 GPU (16G).

### 5.3. Model Comparison (RQ1)

To compare the performance of all methods, we perform disease or gender prediction (i.e., brain network classification) tasks on eight real-world datasets. Moreover, we use average accuracy and AUC score as measurement metrics. Considering that some baselines are challenging to deal with the initial weighted matrices of the brain networks that are almost complete graphs, we perform representation learning for all methods on adjacency matrices generated by the network building module. Taking GCN as an example, Fig. 2 visualizes the transformation process of the adjacency matrices of two subjects from the HIV-fMRI and BP-fMRI. According to the experimental results shown in Table 3, we draw the following conclusions:

1) BN-GNN always obtains the highest average accuracy value on all datasets, proving that its brain network representation performance is better than other methods. Specifically, the classification accuracy of BN-GNN on eight datasets is about 2.0% higher than the second-best method on average. 2) All GNN-based methods outperform traditional network representation methods (i.e., DeepWalk and Node2Vec). This phenomenon is expected because the GNN architecture can better capture the local structural information of the network, which is essential for improving the quality of representation learning. In addition, in brain network classification tasks, end-to-end learning strategies in brain network classification tasks are often superior to unsupervised representation learning methods. 3) GAT-based methods are generally better than GCN-based methods.

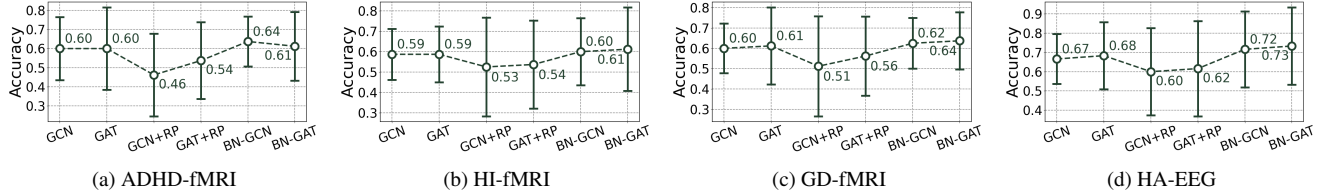


Figure 4: Visualization of ablation experiments to verify the performance of the meta-policy module on four datasets, where GCN+RP and GAT+RP apply a random-policy instead of the meta-policy to guide the aggregation process of GCN and GAT.

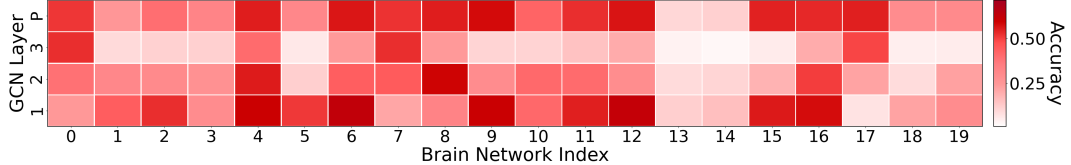


Figure 5: Visualization of the classification results of 20 brain networks randomly sampled from the BP-DTI dataset. From bottom to top, the  $y$ -axis represents the GCN with  $y$  layers and the GCN guided by the meta-policy. The  $x$ -axis represents the network instance index. The colors from light to dark represent the average accuracy from low to high.

Compared with the latter, when the number of layers exceeds two, the performance of the former is usually not greatly degraded. This is because the attention mechanism included in GAT alleviates the over-smoothing problem on some datasets. 4) GNNs combined with skip-connections (i.e., GCN+skip and GAT+skip) do not always enable deeper neural networks to perform better. Compared with the best GCN and GAT models (in the second and third part of Table 3), our BN-GCN and BN-GAT have an average accuracy improvement of 2.5% and 2.1% on eight classification tasks, respectively. Although these observations reveal the limitations of skip-connections, they also confirm the hypothesis of this work that different brain networks require different aggregation iterations. In other words, since the brain networks of real subjects are usually different, customizing different GNN architectures for different subjects is essential to improve network representation performance and provide therapeutic intervention. 5) Though GraphSAGE and FastGCN improve the efficiency or structure information mining capability of the original GCN, their performance is still inferior to our BN-GNN. This phenomenon indicates that searching suitable feature aggregation strategies for network instances in brain network analysis may be more important than exploring sampling or structural reconstruction strategies.

#### 5.4. Ablation Study (RQ2)

The classification results and analysis in Sec. 5.3 confirm the superiority of GNN-based methods in processing brain network data. Furthermore, we conduct ablation studies to explore the specific impact of the network building module and the meta-policy module included in the proposed BN-GNN on the above classification tasks. Specifically, for the network building module, we compare the classification results based on the initial weighted matrices and processed adjacency matrices on BP-fMRI and HIV-fMRI, respectively. For the meta-policy module, we compare the performance difference between BN-GNN and GNN based on random-policy on four datasets.

Fig. 3 visualizes the accuracy and AUC scores of ablation studies for network building, from which we draw the following observations: 1) Utilizing the adjacency matrices generated by the network building module to replace the initial weighted matrices greatly improves the classification performance of the GNN-based methods under the two metrics. This phenomenon indicates that our proposed network building module is beneficial to promote the application of GNN in the field of brain network research. 2) The performance of SDBN on the initial matrices is better than that on the adjacency matrices. On the one hand, SDBN reconstructs the brain networks and enhance the spatial structure information of the initial weighted matrices, thereby enabling the CNN to capture the highly non-linear features. On the other hand, the sparse adjacency matrices generated by the network building module may not be suitable for CNN-based methods. It is worth noting that the optimal performance of SDBN is always inferior to that of BN-GNN, indicating that it is meaningful to learn topological brain networks based on GNN. 3) Even though GAT-based methods (including PR-GNN and GAT) use the attention mechanism to learn the importance of different neighbors, they are still difficult to deal with densely connected initial brain networks. Thus, generating adjacency matrices (as shown in Fig. 2) for GNN is essential to improve the learning of brain network representation.

We replace the meta-policy module in BN-GNN with a random-policy (randomly chooses an action for a given instance) to construct the baselines of ablation experiments, namely GCN+RP and GAT+RP. Fig. 4 and Fig. 5 illustrate the results of ablation experiments for the meta-policy module, from which we draw the following observations: 1) The performance of GCN+RP and GAT+RP are worse than BN-GNN and original GNNs on ADHD-fMRI, HI-fMRI, GD-fMRI, and HA-EEG.

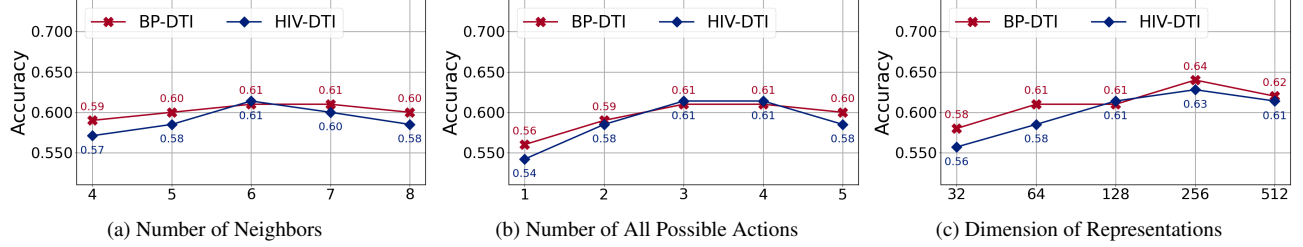


Figure 6: Hyperparameter sensitivity analysis of BN-GNN on the two datasets.

2) Our BN-GNN is better than the original GNNs. In order to explore how the meta-policy improves the original GNN, we illustrate the classification performance of GCNs with a fixed number of layers and the GCN guided by the meta-policy on the BP-DTI dataset in Fig. 5. We observe that different brain networks require different times of feature aggregation, and the meta-policy always make accurate judgments. These observations verify the effectiveness of the meta-policy module.

### 5.5. Hyperparameter Analysis (RQ3)

We study the impact of important hyperparameters in the three modules of BN-GNN, namely the number of neighbors in the network building module, the number of all possible actions in the meta-policy module, and the dimension of network representations in the GNN module. Fig. 6(a) shows that increasing the number of neighbors (determined by  $k$  of KNN) when building the adjacency matrix does not always yield better network representations. The possible reason is that each region in the brain network only has meaningful connections with a limited number of neighbors. From Fig. 6(b), we observe that the performance of BN-GNN is often the best when the number of aggregations is 3. When the action space is further expanded, BN-GNN still maintains a relatively stable performance. These two phenomena verify that the best representation of most brain networks can be obtained within 3 aggregations, and BN-GNN is robust to the setting of the action space size (i.e., the number of all possible actions, which is equal to the maximum number of aggregations that may occur). The results in Fig. 6(c) show that unless the dimension is too small, the performance of BN-GNN will not be excessively affected by the change of the representation dimension.

## 6. Conclusions

In this paper, we propose a novel GNN-based network representation learning framework for brain network analysis, namely BN-GNN. To the best of our knowledge, BN-GNN is the first framework that applies DRL and GNN to achieve customized aggregation for different networks, effectively improving traditional GNNs in brain network representation learning. Experimental results show that the proposed BN-GNN consistently outperforms state-of-the-art baselines on eight real-world brain network datasets. In future work, we will continue to focus on exploring the customized analysis of brain networks for different subjects, such as introducing multi-agent reinforcement learning in GNN-based brain analysis.

## Acknowledgment

The authors of this paper were supported by the National Key R&D Program of China through grant 2021YFB1714800, NSFC through grants U20B2053 and 62073012, S&T Program of Hebei through grant 20310101D, Lehigh's Accelerator Program through grant S00010293. NSF under grants III-1763325, III-1909323, SaTC-1930941, and ONR N00014-18-1-2009.

## References

- [1] A. L. Alexander, J. E. Lee, M. Lazar, A. S. Field, Diffusion tensor imaging of the brain, *Neurotherapeutics* 4 (2007) 316–329.
- [2] S. A. Huettel, A. W. Song, G. McCarthy, et al., *Functional magnetic resonance imaging*, volume 1, Sinauer Associates Sunderland, MA, 2004.
- [3] M. P. Van Den Heuvel, H. E. H. Pol, Exploring the brain network: A review on resting-state fmri functional connectivity, *European Neuropsychopharmacology* 20 (2010) 519–534.

[4] M. Urbanski, M. T. De Schotten, S. Rodrigo, et al., Brain networks of spatial awareness: Evidence from diffusion tensor imaging tractography, *Journal of Neurology Neurosurgery and Psychiatry* 79 (2008) 598–601.

[5] Y. Liu, L. He, B. Cao, P. S. Yu, A. B. Ragin, A. D. Leow, Multi-view multi-graph embedding for brain network clustering analysis, in: *Proceedings of the AAAI Conference on Artificial Intelligence*, volume 32, AAAI Press, 2018, pp. 117–124.

[6] S. Parisot, S. I. Ktena, E. Ferrante, M. Lee, R. Guerrero, B. Glocker, D. Rueckert, Disease prediction using graph convolutional networks: Application to autism spectrum disorder and alzheimer’s disease, *Medical Image Analysis* 48 (2018) 117–130.

[7] H. Braak, E. Braak, Neuropathological staging of alzheimer-related changes, *Acta Neuropathologica* 82 (1991) 239–259.

[8] X. Zhang, L. He, K. Chen, Y. Luo, J. Zhou, F. Wang, Multi-view graph convolutional network and its applications on neuroimage analysis for parkinson’s disease, in: *AMIA Annual Symposium Proceedings*, volume 2018, American Medical Informatics Association, 2018, pp. 1147–1156.

[9] Y. Huang, L. Mucke, Alzheimer mechanisms and therapeutic strategies, *Cell* 148 (2012) 1204–1222.

[10] B. Cao, L. He, X. Wei, M. Xing, P. S. Yu, H. Klumpp, A. D. Leow, t-bne: Tensor-based brain network embedding, in: *International Conference on Data Mining*, SIAM, 2017, pp. 189–197.

[11] T. N. Kipf, M. Welling, Semi-supervised classification with graph convolutional networks, in: *International Conference on Learning Representations*, 2017.

[12] P. Velickovic, G. Cucurull, A. Casanova, A. Romero, P. Lio, Y. Bengio, Graph attention networks, in: *International Conference on Learning Representations*, 2018.

[13] W. L. Hamilton, Z. Ying, J. Leskovec, Inductive representation learning on large graphs, in: *NeurIPS*, 2017, pp. 1025–1035.

[14] Y. LeCun, Y. Bengio, G. Hinton, Deep learning, *Nature* 521 (2015) 436–444.

[15] X. Ma, J. Wu, S. Xue, J. Yang, C. Zhou, Q. Z. Sheng, H. Xiong, L. Akoglu, A comprehensive survey on graph anomaly detection with deep learning, *IEEE Transactions on Knowledge and Data Engineering* (2021).

[16] F. Liu, S. Xue, J. Wu, C. Zhou, W. Hu, C. Paris, S. Nepal, J. Yang, P. S. Yu, Deep learning for community detection: Progress, challenges and opportunities, in: *International Joint Conference on Artificial Intelligence*, 2020, pp. 4981–4987.

[17] H. Peng, J. Li, Q. Gong, Y. Ning, S. Wang, L. He, Motif-matching based subgraph-level attentional convolutional network for graph classification, in: *Proceedings of the AAAI Conference on Artificial Intelligence*, volume 34, 2020, pp. 5387–5394.

[18] Q. Sun, J. Li, H. Peng, J. Wu, Y. Ning, P. S. Yu, L. He, Sugar: Subgraph neural network with reinforcement pooling and self-supervised mutual information mechanism, in: *Proceedings of the Web Conference*, 2021, pp. 2081–2091.

[19] S. Arslan, S. I. Ktena, B. Glocker, D. Rueckert, Graph saliency maps through spectral convolutional networks: Application to sex classification with brain connectivity, in: *Graphs in Biomedical Image Analysis and Integrating Medical Imaging and Non-Imaging Modalities*, Springer, 2018, pp. 3–13.

[20] S. I. Ktena, S. Parisot, E. Ferrante, M. Rajchl, M. Lee, B. Glocker, D. Rueckert, Metric learning with spectral graph convolutions on brain connectivity networks, *NeuroImage* 169 (2018) 431–442.

[21] K. Oono, T. Suzuki, Graph neural networks exponentially lose expressive power for node classification, in: *International Conference on Learning Representations*, 2019.

[22] D. Chen, Y. Lin, W. Li, P. Li, J. Zhou, X. Sun, Measuring and relieving the over-smoothing problem for graph neural networks from the topological view, in: *Proceedings of the AAAI Conference on Artificial Intelligence*, volume 34, 2020, pp. 3438–3445.

[23] H. Gao, S. Ji, Graph u-nets, in: *International Conference on Machine Learning*, PMLR, 2019, pp. 2083–2092.

[24] G. Li, M. Muller, A. Thabet, B. Ghanem, Deepgcns: Can gcns go as deep as cnns?, in: Proceedings of the IEEE/CVF International Conference on Computer Vision, 2019, pp. 9267–9276.

[25] K.-H. Lai, D. Zha, K. Zhou, X. Hu, Policy-gnn: Aggregation optimization for graph neural networks, in: Proceedings of the ACM SIGKDD International Conference on Knowledge Discovery Data Mining, 2020, pp. 461–471.

[26] D. Zha, K.-H. Lai, K. Zhou, X. Hu, Experience replay optimization, in: International Joint Conference on Artificial Intelligence, 2019.

[27] V. Mnih, K. Kavukcuoglu, D. Silver, A. A. Rusu, J. Veness, M. G. Bellemare, A. Graves, M. Riedmiller, A. K. Fidjeland, G. Ostrovski, et al., Human-level control through deep reinforcement learning, *Nature* 518 (2015) 529–533.

[28] H. Van Hasselt, A. Guez, D. Silver, Deep reinforcement learning with double q-learning, in: Proceedings of the AAAI Conference on Artificial Intelligence, volume 30, 2016.

[29] K. Arulkumaran, M. P. Deisenroth, M. Brundage, A. A. Bharath, Deep reinforcement learning: A brief survey, *IEEE Signal Processing Magazine* 34 (2017) 26–38.

[30] H. Peng, J. Li, Y. Song, R. Yang, R. Ranjan, P. S. Yu, L. He, Streaming social event detection and evolution discovery in heterogeneous information networks, *ACM Transactions on Knowledge Discovery from Data (TKDD)* 15 (2021) 1–33.

[31] H. Peng, R. Yang, Z. Wang, J. Li, L. He, P. Yu, A. Zomaya, R. Ranjan, Lime: Low-cost incremental learning for dynamic heterogeneous information networks, *IEEE Transactions on Computers* (2021).

[32] J. Sun, J. Zhang, Q. Li, X. Yi, Y. Liang, Y. Zheng, Predicting citywide crowd flows in irregular regions using multi-view graph convolutional networks, *IEEE Transactions on Knowledge and Data Engineering* (2020).

[33] H. Peng, B. Du, M. Liu, M. Liu, S. Ji, S. Wang, X. Zhang, L. He, Dynamic graph convolutional network for long-term traffic flow prediction with reinforcement learning, *Information Sciences* 578 (2021) 401–416.

[34] Z. Liu, X. Li, H. Peng, L. He, P. S. Yu, Heterogeneous similarity graph neural network on electronic health records, in: IEEE International Conference on Big Data, IEEE, 2020, pp. 1196–1205.

[35] Y. Dou, Z. Liu, L. Sun, Y. Deng, H. Peng, P. S. Yu, Enhancing graph neural network-based fraud detectors against camouflaged fraudsters, in: Proceedings of the ACM International Conference on Information Knowledge Management, 2020, pp. 315–324.

[36] H. Peng, R. Zhang, Y. Dou, R. Yang, J. Zhang, P. S. Yu, Reinforced neighborhood selection guided multi-relational graph neural networks, *ACM Transactions on Information Systems* (2021) 1–46.

[37] H. Peng, R. Zhang, S. Li, Y. Cao, S. Pan, P. Yu, Reinforced, incremental and cross-lingual event detection from social messages, *IEEE Transactions on Pattern Analysis and Machine Intelligence* (2022) 1–1.

[38] Y. Gao, H. Yang, P. Zhang, C. Zhou, Y. Hu, Graph neural architecture search., in: International Joint Conference on Artificial Intelligence, volume 20, 2020, pp. 1403–1409.

[39] T. Nishi, K. Otaki, K. Hayakawa, T. Yoshimura, Traffic signal control based on reinforcement learning with graph convolutional neural nets, in: International Conference on Intelligent Transportation Systems, IEEE, 2018, pp. 877–883.

[40] Z. Yan, J. Ge, Y. Wu, L. Li, T. Li, Automatic virtual network embedding: A deep reinforcement learning approach with graph convolutional networks, *IEEE Journal on Selected Areas in Communications* 38 (2020) 1040–1057.

[41] X. Li, Y. Zhou, N. C. Dvornek, M. Zhang, J. Zhuang, P. Ventola, J. S. Duncan, Pooling regularized graph neural network for fmri biomarker analysis, in: International Conference on Medical Image Computing and Computer-Assisted Intervention, Springer, 2020, pp. 625–635.

[42] X. Bi, Z. Liu, Y. He, X. Zhao, Y. Sun, H. Liu, Gnea: A graph neural network with elm aggregator for brain network classification, *Complexity* 2020 (2020).

[43] H. Jiang, P. Cao, M. Xu, J. Yang, O. Zaiane, Hi-gcn: A hierarchical graph convolution network for graph embedding learning of brain network and brain disorders prediction, *Computers in Biology and Medicine* 127 (2020) 104096.

[44] G. Ma, N. K. Ahmed, T. L. Willke, D. Sengupta, M. W. Cole, N. B. Turk-Browne, P. S. Yu, Deep graph similarity learning for brain data analysis, in: Proceedings of the ACM International Conference on Information and Knowledge Management, 2019, pp. 2743–2751.

[45] P. Zhong, D. Wang, C. Miao, Eeg-based emotion recognition using regularized graph neural networks, *IEEE Transactions on Affective Computing* (2020) 1–1.

[46] X. Xing, Q. Li, M. Yuan, H. Wei, Z. Xue, T. Wang, F. Shi, D. Shen, Ds-gcns: Connectome classification using dynamic spectral graph convolution networks with assistant task training, *Cerebral Cortex* 31 (2021) 1259–1269.

[47] M. B. Gurbuz, I. Rekik, Mgn-net: A multi-view graph normalizer for integrating heterogeneous biological network populations, *Medical Image Analysis* 71 (2021) 102059.

[48] Y. Zhang, H. Huang, New graph-blind convolutional network for brain connectome data analysis, in: International Conference on Information Processing in Medical Imaging, Springer, 2019, pp. 669–681.

[49] A. B. Ragin, H. Du, R. Ochs, Y. Wu, C. L. Sammet, A. Shoukry, L. G. Epstein, Structural brain alterations can be detected early in hiv infection, *Neurology* 79 (2012) 2328–2334.

[50] G. Ma, L. He, C.-T. Lu, W. Shao, P. S. Yu, A. D. Leow, A. B. Ragin, Multi-view clustering with graph embedding for connectome analysis, in: Proceedings of the ACM International Conference on Information Knowledge Management, 2017, pp. 127–136.

[51] C. Yan, Y. Zang, Dparsf: A matlab toolbox for "pipeline" data analysis of resting-state fmri, *Frontiers in systems neuroscience* 4 (2010) 13.

[52] N. Tzourio-Mazoyer, B. Landeau, D. Papathanassiou, F. Crivello, O. Etard, N. Delcroix, B. Mazoyer, M. Joliot, Automated anatomical labeling of activations in spm using a macroscopic anatomical parcellation of the mni mri single-subject brain, *Neuroimage* 15 (2002) 273–289.

[53] S. M. Smith, M. Jenkinson, M. W. Woolrich, C. F. Beckmann, T. E. Behrens, H. Johansen-Berg, P. R. Bannister, M. De Luca, I. Drobniak, D. E. Flitney, et al., Advances in functional and structural mr image analysis and implementation as fsl, *Neuroimage* 23 (2004) S208–S219.

[54] B. Cao, L. Zhan, X. Kong, P. S. Yu, N. Vizueta, L. L. Altshuler, A. D. Leow, Identification of discriminative subgraph patterns in fmri brain networks in bipolar affective disorder, in: International Conference on Brain Informatics and Health, Springer, 2015, pp. 105–114.

[55] S. Whitfield-Gabrieli, A. Nieto-Castanon, Conn: A functional connectivity toolbox for correlated and anticorrelated brain networks, *Brain Connectivity* 2 (2012) 125–141.

[56] R. C. Craddock, G. A. James, P. E. Holtzheimer III, X. P. Hu, H. S. Mayberg, A whole brain fmri atlas generated via spatially constrained spectral clustering, *Human Brain Mapping* 33 (2012) 1914–1928.

[57] S. Pan, J. Wu, X. Zhu, G. Long, C. Zhang, Task sensitive feature exploration and learning for multitask graph classification, *IEEE Transactions on Cybernetics* 47 (2016) 744–758.

[58] H. Hernandez-Perez, J. Mikiel-Hunter, D. McAlpine, S. Dhar, S. Boothalingam, J. J. Monaghan, C. M. McMahon, Perceptual gating of a brainstem reflex facilitates speech understanding in human listeners, *bioRxiv* (2021) 2020–05.

[59] R. Oostenveld, P. Fries, E. Maris, J.-M. Schoffelen, Fieldtrip: Open source software for advanced analysis of meg, eeg, and invasive electrophysiological data, *Computational Intelligence and Neuroscience* 2011 (2011).

[60] G. Nolte, O. Bai, L. Wheaton, Z. Mari, S. Vorbach, M. Hallett, Identifying true brain interaction from eeg data using the imaginary part of coherency, *Clinical Neurophysiology* 115 (2004) 2292–2307.

[61] B. Perozzi, R. Al-Rfou, S. Skiena, Deepwalk: Online learning of social representations, in: Proceedings of the ACM SIGKDD International Conference on Knowledge Discovery Data Mining, 2014, pp. 701–710.

[62] A. Grover, J. Leskovec, Node2vec: Scalable feature learning for networks, in: Proceedings of the ACM SIGKDD International Conference on Knowledge Discovery Data Mining, 2016, pp. 855–864.

[63] T. Mikolov, K. Chen, G. Corrado, J. Dean, Efficient estimation of word representations in vector space, in: International Conference on Learning Representations, 2013.

- [64] J. Chen, T. Ma, C. Xiao, Fastgcn: Fast learning with graph convolutional networks via importance sampling, in: International Conference on Learning Representations, 2018.
- [65] S. Wang, L. He, B. Cao, C.-T. Lu, P. S. Yu, A. B. Ragin, Structural deep brain network mining, in: Proceedings of the ACM SIGKDD International Conference on Knowledge Discovery Data Mining, 2017, pp. 475–484.
- [66] A. Krizhevsky, I. Sutskever, G. E. Hinton, Imagenet classification with deep convolutional neural networks, *Advances in Neural Information Processing Systems* 25 (2012) 1097–1105.